

Local origin of global contact numbers in frictional ellipsoid packings

Fabian M. Schaller,^{1,2,*} Max Neudecker,² Mohammad Saadatfar,³ Gary W. Delaney,⁴ Gerd E. Schröder-Turk,^{1,†} and Matthias Schröder^{2,‡}

¹*Institut für Theoretische Physik, Friedrich-Alexander-Universität Erlangen-Nürnberg, 91058 Erlangen, Germany*

²*Max Planck Institute for Dynamics and Self-Organization (MPIDS), 37077 Goettingen, Germany*

³*Applied Maths, RSPHysSE, The Australian National University, Australia*

⁴*CSIRO Mathematics, Informatics and Statistics, Clayton South, Victoria, Australia*

(Dated: October 29, 2018)

In particulate soft matter systems the average number of contacts Z of a particle is an important predictor of the mechanical properties of the system. Using X-ray tomography, we analyze packings of frictional, oblate ellipsoids of various aspect ratios α , prepared at different global volume fractions ϕ_g . We find that Z is a monotonously increasing function of ϕ_g for all α . We demonstrate that this functional dependence can be explained by a local analysis where each particle is described by its local volume fraction ϕ_l computed from a Voronoi tessellation. Z can be expressed as an integral over all values of ϕ_l : $Z(\phi_g, \alpha, X) = \int Z_l(\phi_l, \alpha, X) P(\phi_l|\phi_g) d\phi_l$. The local contact number function $Z_l(\phi_l, \alpha, X)$ describes the relevant physics in term of locally defined variables only, including possible higher order terms X . The conditional probability $P(\phi_l|\phi_g)$ to find a specific value of ϕ_l given a global packing fraction ϕ_g is found to be independent of α and X . Our results demonstrate that for frictional particles a local approach is not only a theoretical requirement but also feasible.

PACS numbers: 45.70.-n,45.70.Cc,61.43.-j,81.70.Tx

The average number of contacts Z that a particle forms with its neighbors is the basic control parameter in the theory of particulate systems known as the jamming paradigm [1, 2] where Z is a function of the difference between the global volume fraction ϕ_g and some critical value ϕ_c . For soft, frictionless spheres (a practical example would be an emulsion) this is indeed a good description [3] because additional contacts are formed by the globally isotropic compression of the particles which also increases ϕ_g . However, in frictional granular media such as sand, salt, or sugar the control of ϕ_g is not achieved by compression but by changing the geometric structure of the sample; if we want to fill more grains into a storage container we do not compress them with a piston, but we tap the container a couple of times on the counter top.

But if Z and ϕ_g are not simultaneously controlled by a globally defined parameter such as pressure, the idea of a function $Z(\phi_g)$ runs into an epistemological problem: contacts are formed at the scale of individual particles and their neighbors. At this scale the global ϕ_g is not only undefined; it would even be impossible for a particle scale demon to compute ϕ_g by averaging over the volume of the neighboring particles. The spatial correlations between Voronoi volumes [4–6] would require it to gather information from a significantly larger volume than the direct neighbors.

To date, only two theoretical approaches have studied Z from a local perspective: Song *et al.* [7] used a mean-field ansatz to derive a functional dependence between Z and the Voronoi volume of a sphere. This ansatz has recently been expanded to arbitrary shapes composed of the unions and intersections of frictionless spheres [8, 9]. Secondly, Clusel *et al.* [10, 11] developed the granocentric model which predicts the probability distribution of

contacts in jammed, polydisperse emulsions. The applicability of the granocentric model to frictional discs has been shown in [12].

The aim of this experimental study is to go beyond spheres and understand how the average Z in packings of frictional ellipsoids originates from the local physics at the grain level. We find that, to a first approximation, the number of contacts an individual particle forms depends on only two parameters: the material parameter α which is the length ratio between the short and the two (identical) long axes of the ellipsoids. And a parameter that characterizes the cage formed by all the neighboring particles: the local volume fraction ϕ_l which is the particle volume divided by the volume of its Voronoi cell.

Frictional ellipsoids used in experiments [13–16] exhibit a number of differences to the frictionless ellipsoids often studied numerically [17–23]. The latter have been found to form packings with less than the number of contacts required for isostaticity, which is defined as having enough constraints to block all degrees of freedom of the particles [17, 21, 24]. This apparent paradox has been resolved by Donev *et al.* [25], who showed that in this analysis the contacts can not be treated as the contacts between frictionless spheres: the curvature of the ellipsoids blocks rotational degrees of freedom even in the absence of friction. In contrast, we find packings of frictional ellipsoids to be hyperstatic over the whole range of ϕ_g studied, in agreement with numerical simulation including friction [26, 27].

Particles and preparation.— We study two different types of oblate ellipsoids, the properties of which are summarized in table I. Figure 1 a) shows pharmaceutical placebo pills (PPP) with $\alpha = 0.59$ produced by Weimer Pharma GmbH. Due to their sugar coating, their sur-

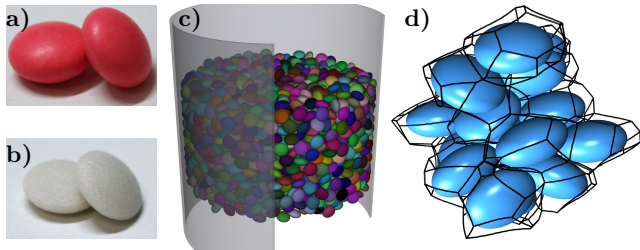


FIG. 1. a) Pharmaceutical placebo pills with $\alpha = 0.59$. b) Gypsum particles made with a 3D printer with $\alpha = 0.40$. c) Rendering of the particles detected in a X-ray tomogram. d) The black wire frame indicates the Voronoi cells of the ellipsoids.

face is rather smooth; their static coefficient of friction μ_s against paper is 0.38 (measured using a small sledge on a slowly raised inclined plane). The second particle type displayed in figure 1 b) are gypsum ellipsoids cured with resin, produced with a 3D printer (Zprinter 650, Z corporation). The aspect ratio of these 3DP particles ranges from 0.4 to 1 (i.e. spherical), their rougher surface results in values of μ_s between 0.67 and 0.75. Due to the production process, the 3DP particles have hummocks of up to 100 μm on their short axis. As a consequence their volume deviates up to 3% from a perfect ellipsoid, compared to 1% for the PPP particles.

Samples are prepared by first creating a loose packing of ellipsoids inside a plexiglass cylinder with an inner diameter of 104 mm; then the samples are tapped in order to increase ϕ_g to the desired value. We use three different protocols to prepare the initial loose samples, they are indicated by different symbols in the figures below. However, our results do not seem to depend on the initial preparation method, details of which can be found in the supplemental material. Except for the loosest samples, the packings are compactified by applying sinusoidally shaped pulses on an electromagnetic shaker (LDS V555). The width of the pulses is 50 ms and the peak acceleration 2 g (where $g = 9.81\text{m/s}^2$). At a repetition rate of 3 Hz up to 1500 taps are applied to prepare the highest values of ϕ_g .

Image analysis. – Tomograms of the prepared packings are acquired using X-ray computed tomography (GE Nanotom) with a resolution of 64 μm per voxel. The resulting three-dimensional gray scale image is the starting point for the identification of all particle centers and orientations (c.f. figure 1c) using the methods described in [28]. To reduce boundary effects, only particles with centers that are at least two long axes away from the container walls were included in our analysis; table I lists the numbers of these core particles. To assure spatial homogeneity, we discard all experiments where the standard deviation of the azimuthally averaged volume fraction is larger than 0.66%. Similarly, to exclude packings with a too large degree of local order we only consider sam-

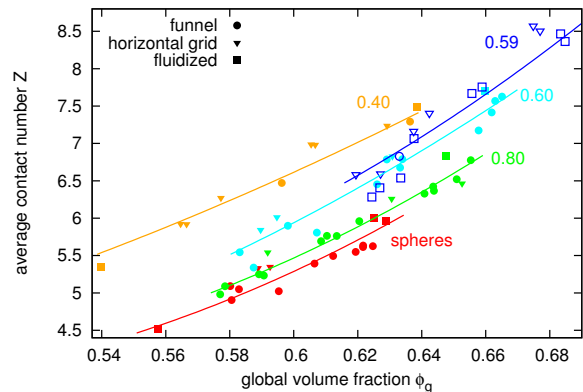


FIG. 2. Contact number as a function of the global volume fraction. Lines correspond to equation 6, which is the numerical integration of the local theory presented here. The different symbols indicate preparation of the initial packing, which is then compactified for all but the loosest samples by tapping. The different aspect ratios and particle types are indicated by different colors, see table I.

ples with $\theta > 0.5$ rad where θ is the average angle of the short axis with respect to gravity with $\theta = 1$ corresponding to a random orientation (see supplemental material). The particle positions and orientations of all experiments reported here can be downloaded from the Dryad repository [29].

From the geometrical representation of the sample we determine the average Z using the contact number scaling method [28]. Finally, the Voronoi cells of the particles are computed with the algorithm described in [30]. Figure 1 d) displays the Voronoi tessellation of a small subset of particles. By dividing the volume of the particle by the volume of the Voronoi cell we obtain for each particle its local volume fraction ϕ_l ; the harmonic mean of all particles in the core region corresponds to the global volume fraction ϕ_g .

The average contact number Z as a function of ϕ_g is displayed in figure 2. The main conclusion of figure 2 is that the global average of Z depends on both ϕ_g and α . As expected for frictional particles [31–35], the contact number of all samples is significantly above the isostatic value of four [36].

Switching to a local ansatz. – As discussed in the introduction, the formation of contacts between particles needs to be explained solely by parameters which are well defined on the particle level. We therefore start with an ansatz:

$$Z(\phi_g, \alpha, X) = \int Z_l(\phi_l, \alpha, X) P(\phi_l | \phi_g, \alpha, X) d\phi_l \quad (1)$$

Here the contact function $Z_l(\phi_l, \alpha, X)$ represents the local physics i.e. the number of contacts formed by a particle of shape α , inside a Voronoi cell of size ϕ_l and potentially characterized by further locally defined variables

aspect ratio α	half axis		type	friction coefficient μ_s	particles in core region	number of analyzed packings	Empirical fit parameters for $Z_l(\phi_l, \alpha)$		
	short [mm]	long [mm]					a	b	c
spheres ●	3.1		3DP	0.75 ± 0.07	660-850	15	60.4	-52.2	14.8
0.80 ●	2.65	3.30	3DP	0.75 ± 0.05	750-850	17	60.4	-52.4	15.1
0.60 ●	2.20	3.75	3DP	0.67 ± 0.03	620-710	16	44.7	-31.0	8.4
0.59 ○	2.15	3.55	PPP	0.38 ± 0.05	850-910	15	63.5	-53.7	15.4
0.40 ●	1.60	4.00	3DP	0.67 ± 0.05	620-730	10	25.3	-10.7	3.9

TABLE I. Material properties of the particles. The first column displays the color code used in figures 2 to 4. Error-bars on μ_s are standard deviations over 15 experiments. The last three columns show the empirical fit parameters for $Z_l(\phi_l, \alpha)$ according to equation 2.

X such as friction, fabric anisotropy, or measures of local order. $P(\phi_l|\phi_g, \alpha, X)$ is the conditional probability to find a particle with ϕ_l in a given packing; an integration over all values of ϕ_l will result in the global value of Z .

In order to measure how Z_l depends on ϕ_l , we determine the local contact number for each ellipsoid, see supplemental material. Figure 3 a) shows $Z_l(\phi_l)$ curves for all our experiments. The main point here is that in agreement with our ansatz the curves for the 3DP particles do not depend on the global volume fraction ϕ_g . This result has been previously only shown for spheres [37]. For the PPP particles the collapse is less conclusive, we discuss possible reasons below. In consequence, we take for each value of α the average over all experiments, the resulting $Z_l(\phi_l, \alpha)$ curves are shown in figure 3 b). Here we have ignored not only ϕ_g but also all higher order terms X because within the resolution of our experiments we were not able to discern between different possible candidates. For a discussion of e.g. X being the orientation of the short axis see the supplemental material. In order to obtain an phenomenological description for Z_l we perform for each aspect ratio a parabola fit using:

$$Z_l(\phi_l, \alpha) = a \phi_l^2 + b \phi_l + c \quad (2)$$

The results are displayed in figure 3 b), the values of the fit parameters a , b , and c are listed in table I.

Fitting equation 2 is a purely phenomenological approach, it is justified only by the absence of any theoretical predictions for frictional ellipsoids. The only analytical result available is for spheres [7], it is in good agreement with our data (without any fit parameters) as shown in the inset of figure 3. However, as discussed in the supplementary material, this result can not be easily generalized to frictional ellipsoids. Also included in the supplemental material are fits which show that even a local re-interpretation of the jamming paradigm does fail to describe the physics.

Properties of the local volume fraction distribution.— Figure 4 reveals a number of interesting scaling properties of $P(\phi_l)$. Panel 4 a) shows $P(\phi_l)$ for all different aspect ratio at $\phi_g \approx 0.625$. The good agreement indicates that $P(\phi_l)$ is independent of α . In figure 4 b) a rescaled P

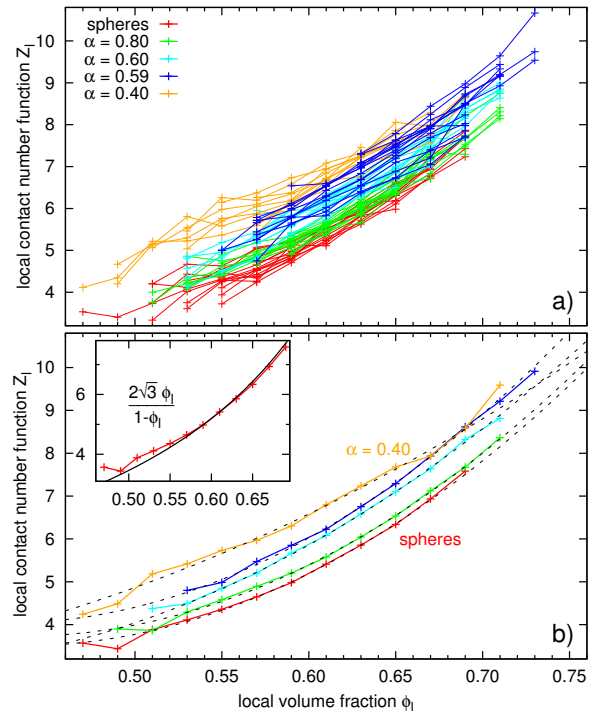


FIG. 3. Measuring the local contact number function Z_l which describes how many contacts an average particle with a local area fraction ϕ_l will form. In panel a) each line corresponds to a single experiment, i.e. a single datapoint in figure 2. Each cross represents the average number of contacts a particle with this value of ϕ_l (using a bin size of 0.02) will form. The colored lines in panel b) are averages over all data sets (i.e. different values of ϕ_g) displayed in the upper panel. The black dashed lines are parabolic fits according to equation 2. The inset shows the theoretical result from Song *et al.* [7] for spheres compared with our sphere data.

is plotted for all values of ϕ_g . This demonstrates, that the mean (aka ϕ_g) and the standard deviation of the local volume fraction distribution $\sigma(\phi_g)$ are sufficient to describe P . This result has previously only been known for spheres [38, 39] and discs [12]. Finally, figure 4 c) demonstrates that the standard deviation $\sigma(\phi_l)$ of the local packing fraction distribution depends only on ϕ_g

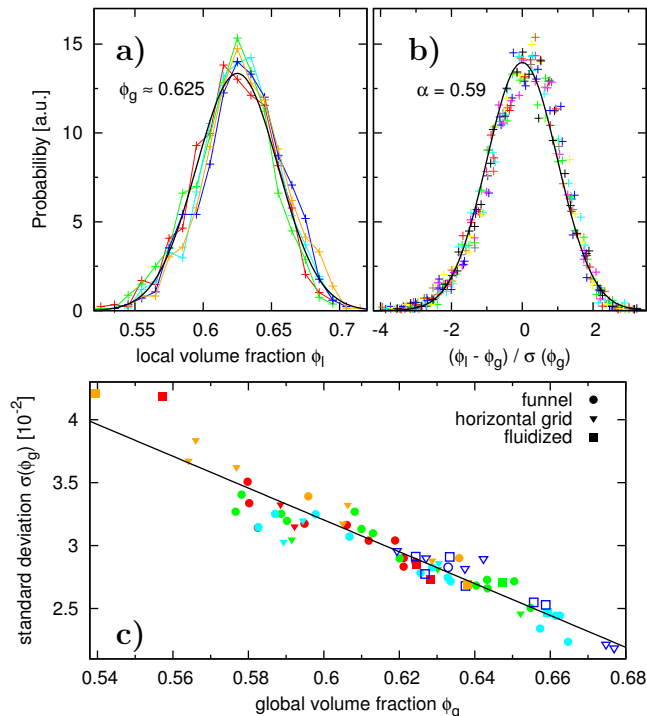


FIG. 4. Scaling properties of the local volume fraction distribution $P(\phi_l)$. a) For a given global volume fraction (here $\phi_g \approx 0.625$) the probability of finding a specific value of ϕ_l does not depend on α . b) P can be rescaled using ϕ_g and the standard deviation of the local volume fractions σ . Shown here are all experiments with $\alpha = 0.59$. The black lines in panels a and b are Gaussian fits using equation 4. c) The standard deviations of the local volume fraction distribution depends only on ϕ_g . Panel includes all experiments shown in figure 2. The black line is a linear fit resulting in equation 5.

and not α .

Together, these results show that $P(\phi_l|\phi_g, \alpha, X)$ in equation 1 can be replaced by $P(\phi_l|\phi_g)$:

$$Z(\phi_g, \alpha, X) = \int Z_l(\phi_l, \alpha, X) P(\phi_l|\phi_g) d\phi_l \quad (3)$$

The advantage of this ansatz is a clear separation of the contact number problem into the local physics at the grain level and a probabilistic term connecting the local and the global volume fraction. Please note that without a better understanding of the origin of the scaling properties shown in figure 4 it is not possible to decide on the causality between ϕ_l and ϕ_g . So writing $P(\phi_l|\phi_g)$ can imply either that ϕ_g is the cause of the observed $P(\phi_l)$ or that ϕ_g can be seen to follow from the prepared $P(\phi_l)$.

In order to get an empirical expression for Z we fit the local packing fraction distribution $P(\phi_l|\phi_g)$ with a Gaussian[40]

$$P(\phi_l|\phi_g) = \frac{1}{\sigma(\phi_g) \sqrt{2\pi}} e^{-\frac{(\phi_l - \phi_g)^2}{2\sigma(\phi_g)^2}} \quad (4)$$

and the dependence of σ on ϕ_g with a linear equation which yields:

$$\sigma(\phi_g) = -0.126 \phi_g + 0.109 \quad (5)$$

Both fits are displayed as black lines in figure 4. Entering equations 2 and 4 into equation 3 and performing the integration leads to:

$$Z(\phi_g, \alpha) = a \sigma(\phi_g)^2 + a \phi_g^2 + b \phi_g + c \quad (6)$$

with σ according to equation 5 and a, b, c as shown in table I.

A comparison of our experimental data with equation 6 is shown in figure 2. The good agreement for all 3DP particles demonstrates the validity of our ansatz equation 3. For the PPP particles with $\alpha = 0.59$ the agreement is only fair, pointing to the need for an additional parameter X in $Z_l(\phi_g, \alpha, X)$. However, the experimental scatter does not allow us to assess the type of higher order corrections required. The need for inclusion of such a parameter can also stem from the history-dependent behavior of frictional particles. It has recently been shown for spheres [41] and tetrahedra [35, 42] that for identical ϕ_g the contact number can depend on the preparation history; modeling such behavior will require the addition of further locally defined parameters.

Conclusion. – The global contact numbers of packings of frictional spheres and ellipsoids can be explained by an ansatz which combines a local contact function and a conditional probability. The contact function does depend solely on parameters defined on the particles scale, including the local volume fraction and the aspect ratio of the particles. The conditional probability to find a particle with a specific local volume fraction is sufficiently described by the global volume fraction alone. We expect our results, available also as open data, to be a valuable reference point for the generalization of existing theoretical approaches such as the granocentric model [10, 11] or the statistical mechanics approach to granular media [7, 8] towards frictional granular matter. Extensions of our contact function including other locally defined parameters, such as e.g. the fabric anisotropy, should be able to describe non-isotropic effects, such as observed in shear-jammed frictional packings [43, 44].

We thank Weimer Pharma GmbH for providing the PPP samples, Martin Brinkmann, Stephan Herminghaus, Marco Mazza, Klaus Mecke and Jean-François Métayer for valuable discussions and Matthias Hoffmann for programming support. We acknowledge funding by the German Science Foundation (DFG) through the research group "Geometry and Physics of Spatial Random Systems" under grant no SCHR-1148/3-1.

* fabian.schaller@physik.uni-erlangen.de

[†] gerd.schroeder-turk@fau.de

[‡] matthias.schroeter@ds.mpg.de

- [1] A. J. Liu and S. R. Nagel, *Ann. Rev. Cond. Matt. Phys.* **1**, 347 (2010).
- [2] M. van Hecke, *J. Phys.: Condens. Matter* **22**, 033101 (2010).
- [3] G. Katgert and M. v. Hecke, *Europhys. Lett.* **92**, 34002 (2010).
- [4] F. Lechenault, F. d. Cruz, O. Dauchot, and E. Bertin, *J. Stat. Mech.* **2006**, P07009 (2006).
- [5] S.-C. Zhao, S. Sidle, H. L. Swinney, and M. Schröter, *Europhys. Lett.* **97**, 34004 (2012).
- [6] S.-C. Zhao, *Length scales in granular matter*, Ph.D. thesis, Georg-August University Göttingen (2013).
- [7] C. Song, P. Wang, and H. A. Makse, *Nature* **453**, 629 (2008).
- [8] A. Baule, R. Mari, L. Bo, L. Portal, and H. A. Makse, *Nature Comm.* **4**, 2194 (2013).
- [9] A. Baule and H. A. Makse, *Soft Matter* **10**, 4423 (2014).
- [10] M. Clusel, E. I. Corwin, A. O. N. Siemens, and J. Brujić, *Nature* **460**, 611 (2009).
- [11] E. I. Corwin, M. Clusel, A. O. N. Siemens, and J. Brujić, *Soft Matter* **6**, 2949 (2010).
- [12] J. G. Puckett, F. Lechenault, and K. E. Daniels, *Phys. Rev. E* **83**, 041301 (2011).
- [13] W. Man, A. Donev, F. H. Stillinger, M. T. Sullivan, W. B. Russel, D. Heeger, S. Inati, S. Torquato, and P. M. Chaikin, *Phys. Rev. Lett.* **94**, 198001 (2005).
- [14] S. Farhadi and R. P. Behringer, *Phys. Rev. Lett.* **112**, 148301 (2014).
- [15] C. Xia, K. Zhu, Y. Cao, H. Sun, B. Kou, and Y. Wang, *Soft Matter* **10**, 990 (2014).
- [16] S. Wegner, R. Stannarius, A. Boese, G. Rose, B. Szabó, E. Somfai, and T. Börzsönyi, *Soft Matter* **10**, 5157 (2014).
- [17] A. Donev, I. Cisse, D. Sachs, E. A. Variano, F. H. Stillinger, R. Connelly, S. Torquato, and P. M. Chaikin, *Science* **303**, 990 (2004).
- [18] A. Donev, F. H. Stillinger, P. M. Chaikin, and S. Torquato, *Phys. Rev. Lett.* **92**, 255506 (2004).
- [19] M. Mailman, C. F. Schreck, C. S. O'Hern, and B. Chakraborty, *Phys. Rev. Lett.* **102**, 255501 (2009).
- [20] Z. Zeravcic, N. Xu, A. J. Liu, S. R. Nagel, and W. v. Saarloos, *Europhys. Lett.* **87**, 26001 (2009).
- [21] C. F. Schreck, N. Xu, and C. S. O'Hern, *Soft Matter* **6**, 2960 (2010).
- [22] S. K. Mkhonta, D. Vernon, K. R. Elder, and M. Grant, *Europhys. Lett.* **101**, 56004 (2013).
- [23] O. Stenzel, M. Salzer, V. Schmidt, P. W. Cleary, and G. W. Delaney, *Granular Matter* **16**, 457 (2014).
- [24] R. M. Baram and P. G. Lind, *Phys. Rev. E* **85**, 041301 (2012).
- [25] A. Donev, R. Connelly, F. H. Stillinger, and S. Torquato, *Phys. Rev. E* **75**, 051304 (2007).
- [26] R. Guises, J. Xiang, J.-P. Latham, and A. Munjiza, *Gran. Matt.* **11**, 281 (2009).
- [27] G. W. Delaney, J. E. Hilton, and P. W. Cleary, *Phys. Rev. E* **83**, 051305 (2011).
- [28] F. M. Schaller, M. Neudecker, M. Saadatfar, G. Delaney, K. Mecke, G. E. Schröder-Turk, and M. Schröter, *AIP Conf. Proc.* **1542**, 377 (2013).
- [29] DOI from Dryad, data upload is only possible after paper is accepted by a journal.
- [30] F. M. Schaller, S. C. Kapfer, M. E. Evans, M. J. Hoffmann, T. Aste, M. Saadatfar, K. Mecke, G. W. Delaney, and G. E. Schröder-Turk, *Philosoph. Mag.* **93**, 3993 (2013).
- [31] L. E. Silbert, D. Ertas, G. S. Grest, T. C. Halsey, and D. Levine, *Phys. Rev. E* **65**, 031304 (2002).
- [32] H. P. Zhang and H. A. Makse, *Phys. Rev. E* **72**, 011301 (2005).
- [33] K. Shundyak, M. van Hecke, and W. van Saarloos, *Phys. Rev. E* **75**, 010301 (2007).
- [34] S. Henkes, M. van Hecke, and W. van Saarloos, *Europhys. Lett.* **90**, 14003 (2010).
- [35] M. Neudecker, S. Ulrich, S. Herminghaus, and M. Schröter, *Phys. Rev. Lett.* **111**, 028001 (2013).
- [36] Frictional contacts fix three force components, one normal and two tangential. These are shared between the two particles involved, so per particle each contact provides 1.5 constraints. As each particle possesses six degrees of freedom, at minimum four contacts are needed to block all of them.
- [37] T. Aste, M. Saadatfar, and T. J. Senden, *J. Stat. Mech.: Theory and Exp.* **2006**, P07010 (2006).
- [38] T. Aste, T. D. Matteo, M. Saadatfar, T. J. Senden, M. Schröter, and H. L. Swinney, *Europhys. Lett.* **79**, 24003 (2007).
- [39] F. W. Starr, S. Sastry, J. F. Douglas, and S. C. Glotzer, *Phys. Rev. Lett.* **89**, 125501 (2002).
- [40] We approximate $P(\phi_i|\phi_g)$ by a Gauss function, as this allows explicit integration of equation 2 leading to 6. Note the differences to the k -Gamma distributions [38] for the Voronoi cell volumes of spheres (that require the minimal possible Voronoi volume as an additional parameter, unknown for ellipsoids) are small.
- [41] I. Agnolin and J.-N. Roux, *Phys. Rev. E* **76**, 061302 (2007).
- [42] N. N. Thyagu, M. Neudecker, and M. Schröter, *arXiv:1501.04472* (2015).
- [43] D. Bi, J. Zhang, B. Chakraborty, and R. P. Behringer, *Nature* **480**, 355 (2011).
- [44] M. Grob, C. Heussinger, and A. Zippelius, *Physical Review E* **89**, 050201 (2014).